

---

## **Surface roughness in ultrasonic-assisted and conventional milling of soda-lime glass**

---

**Yasmine El-Taybany\***

Department of Industrial Engineering and Systems Management,  
School of Innovative Design Engineering,  
Egypt-Japan University of Science and Technology,  
P.O. Box 179 New Borg El-Arab City,  
Postcode 21934, Alexandria, Egypt  
Email: yasmine.eltaybany@ejust.edu.eg  
\*Corresponding author

**Mohab Hossam**

Department of Industrial Engineering and Systems Management,  
School of Innovative Design Engineering,  
Egypt-Japan University of Science and Technology,  
P.O. Box 179 New Borg El-Arab City,  
Postcode 21934, Alexandria, Egypt  
Email: mohab.hossam@ejust.edu.eg  
and  
On leave from: Production Engineering Department,  
Faculty of Engineering,  
Alexandria University,  
Alexandria, Egypt

**Jiwang Yan**

Department of Mechanical Engineering,  
Faculty of Science and Technology,  
Keio University,  
Yokohama 2238522, Japan  
Email: yan@mech.keio.ac.jp

**Hassan El-Hofy**

Department of Industrial Engineering and Systems Management,  
School of Innovative Design Engineering,  
Egypt-Japan University of Science and Technology,  
P.O. Box 179 New Borg El-Arab City,  
Postcode 21934, Alexandria, Egypt  
Email: hassan.elhofy@ejust.edu.eg

**Abstract:** Glass has an increasing demand in many industrial fields such as micro-channels and micro reactors in fluidic applications, lab-on-a-chip in medical applications, and micro lens arrays and optical devices. Machining of glass as one of hard-to-machine materials is challengeable due to its distinctive properties of high strength, hardness, and brittleness. Facing these challenges, ultrasonic-assisted milling (UAM); an advanced machining process; was provided for its effectiveness in machining such hard-to-machine materials. In this paper, the effects of feed rate, depth of cut, ultrasonic-vibration assistance, and cutting fluid on surface roughness in UAM of soda-lime glass compared with conventional milling (CM) were investigated. Results showed that, by introducing ultrasonic-vibration, higher surface roughness was obtained. The optimal cutting conditions were attained using response surface methodology. At the optimised parametric setting, the minimum surface roughness was found to be at wet conventional milling.

**Keywords:** ultrasonic-assisted milling; UAM; conventional milling; surface roughness; difficult-to-machine materials; optimisation.

**Reference** to this paper should be made as follows: El-Taybany, Y., Hossam, M., Yan, J. and El-Hofy, H. (2019) 'Surface roughness in ultrasonic-assisted and conventional milling of soda-lime glass', *Int. J. Machining and Machinability of Materials*, Vol. 21, Nos. 1/2, pp.82–99.

**Biographical notes:** Yasmine El-Taybany is a PhD student since 2015 till now at Department of Industrial Engineering and Systems Management, School of Innovative Design Engineering, Egypt-Japan University of Science and Technology, Egypt. She was a research student at precision machining and nano processing – Yan Laboratory, Department of Mechanical Engineering, Faculty of Science and Technology, Keio University, Japan from June 2017 till February 2018. She is an Assistant Lecturer at her home university, Port Said University, Egypt since 2012. Her research interests include machining processes, traditional and non-traditional machining, materials engineering, and production engineering.

Mohab Hossam is an Assistant Professor at the Department of Industrial Engineering and Systems Management, School of Innovative Design Engineering, Egypt. He is currently on leave from Production Engineering Department, Faculty of Engineering, Alexandria University, Alexandria, Egypt. He received his PhD from Department of Machining Technology (ISF), Dortmund University, Germany. His research interests are product design and development, production engineering, engineering drawing, CNC machining, CNC programming, computer aided design, machine tools, and CNC/CAM.

Jiwan Yan is a Full Professor since April 2012 till now at Keio University, Department of Mechanical Engineering, Laboratory for Precision Machining and Nano Processing, Tokyo, Japan. He received his PhD in Precision Engineering from Tohoku University, Japan in 2000, and had been working in Tohoku as an Associate Professor before joining Keio University in April 2012 as a Full Professor. His research interests include micro/nano manufacturing, ultraprecision optical fabrication, surface/subsurface integrity, laser Raman spectroscopy, and laser recovery. He serves as editorial board members for five international journals.

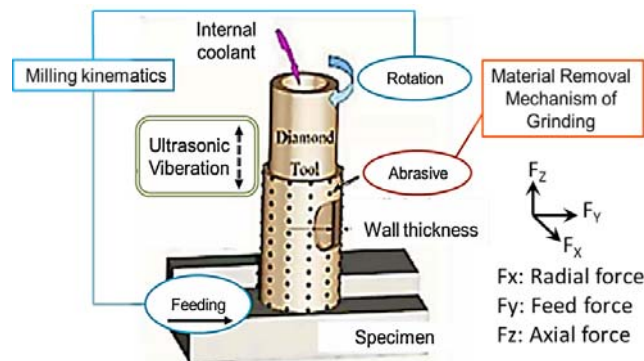
Hassan El-Hofy is a Full Professor since December 2012 till now at the Department of Industrial Engineering and Systems Management, School of Innovative Design Engineering, Egypt-Japan University of Science and Technology, Egypt. He received his PhD from University of Edinburgh, School of Engineering, Edinburgh, UK in 1980–1985. He was the Dean of IDE School at E-JUST, Egypt-Japan University of Science and Technology, Department of Industrial Engineering and Systems Management, Alexandria, Egypt from December 2017 till July 2017. He does research in advanced machining and materials engineering.

## 1 Introduction

Glass offers unique mechanical and physical properties, i.e., high strength, hardness and wear-resistance, that make it increasingly popular in many applications such as optical, biomedical, and electronics industries. Such components require high surface quality and dimensional accuracy as the most specified customer requirements. The major indication of the surface quality of the machined parts is the surface roughness that affects the functional characteristics of the product such as fatigue, fracture-resistance, and surface friction (Dambon et al., 2007; Uhlmann and Hübner, 2007; Feucht et al., 2014; Klocke et al., 2015).

Therefore, machining of glass at high-accuracy and high-efficiency is a challenging task for manufacturers due to its distinctive properties that make it a difficult-to-machine material. Careful selection of the machining parameters is essential and critical in machining such materials which in turn affects the workpiece quality and product performance. Rotary ultrasonic machining (RUM), using an abrasive diamond cutting tool, is recently used as a reliable and cost-effective method of difficult-to-machine materials compared to other non-traditional processes (Feucht et al., 2014; Kumar et al., 2014). Ultrasonic-assisted milling (UAM) is a variation of RUM that combines the milling kinematics with grinding material removal mechanism along with the ultrasonic assistance as shown in Figure 1. The ultrasonic vibration is applied to the cutting tool, which is vibrated vertically along its axis (z-axis).

**Figure 1** Ultrasonic-assisted milling mechanism (see online version for colours)



The literature survey covered the recent researches interested in studying the influence of numerous process parameters, i.e., cutting speed, feed rate, depth of cut, ultrasonic-vibration, and cutting fluid, on the surface roughness during ultrasonic-assisted machining of some difficult-to-machine materials. Jiang et al. (2016) concluded that the surface roughness of K9 optical glass increased by increasing grinding depth, feed rate, and vibration amplitude, but decreased by increasing grinding wheel speed during ultrasonic assisted grinding (UAG). Hu et al. (2017) found that edge chipping, which was detrimental to the surface quality of BK7/K9 glass slots and caused high machining cost, was significantly reduced by the application of ultrasonic vibration. Hamzah et al. (2008) compared the machinability of BK7 optical glass during conventional and rotary ultrasonic drilling in terms of material removal rate (MRR), surface roughness, and chipping size and thickness. However, this comparison was performed at different input variables, different abrasive particle sizes in case of conventional drilling, and different spindle speeds and feed rates in case of RUM leading to unfair comparative results. Another comparison was conducted by Kuo (2008) who stated that the surface roughness of glass milled under non-ultrasonic-assisted condition was lower. Also, the surface roughness of Ni-Alloy was increased in case of ultrasonic vibration-assisted milling (Suárez et al., 2016) and when UAM of CFRP (Abd Halim et al., 2017). Throughout UAM, surface roughness of ceramic material (Jiao et al., 2005; Singh and Singhal, 2017), Ni-Alloy (Suárez et al., 2016), and of CFRP slots (Wang et al., 2017; Ning et al., 2017)) was investigated.

Various statistical modelling techniques were used in RUM. Taguchi methodology was utilised to optimise the surface roughness of milled zirconia ceramic (Abdo et al., 2012), BK7 glass (Lee et al., 2008), SiC (Babuji et al., 2017). Response surface methodology was used to optimise the surface roughness and chipping thickness during RUM of Macor ceramic (Singh and Singhal, 2017); and to optimise the cutting force and surface roughness during rotary ultrasonic face milling of CFRP (Amin et al., 2017).

In the light of the above literature survey, the current work has been focused on experimentally investigating the influence of feed rate, depth of cut, ultrasonic assistance, and cutting fluid on the surface roughness during UAM of soda-lime glass. A comparison between UAM and CM was also reported. Surface finish of the machined products is the major consideration in most industries. To achieve this, proper selection of process parameters is very essential; therefore, optimisation of the selected controllable variables was established to minimise the roughness of the milled surface.

## **2 Materials and methods**

Ultrasonic 20 linear machine (DMG, Germany) was used to conduct slotting experiments. It mainly consists of a high-speed ultrasonic spindle kit with rotation speed up to 42,000 rpm, a water coolant system (internal and external), an HSK32 ultrasonic actuator system, and an integrated NC-swivel rotary table. If the ultrasonic actuator system is shut down, CM could be realised. Soda-lime glass was used as the workpiece material with dimensions of  $30 \times 40 \times 6 \text{ mm}^3$ . The workpiece was clamped with a specially designed fixture mounted on the dynamometer. The experimental setup is shown in Figure 2. Diamond abrasive milling cutter from SCHOTT Ltd Corp., Germany, was used. The specifications of the workpiece material and milling tool are shown in

Tables 1 and 2, respectively. During wet slotting, the cutting fluid (Blaser, Switzerland) was pumped from the centre of the tool at a pressure of 10 bar. In each experiment, a slot was machined with a width equal to the tool diameter ( $\phi$  4 mm) and a length of 30 mm. Prior to slotting tests, a facing process was done for all the specimens to ensure the surface flatness. The surface roughness ( $R_a$  and  $R_z$ ) of the bottom surface of the slot was measured using Ultra-precision point autofocus laser probe-2D (Mitaka, MP-3, Japan). The measurements were conducted at four different positions in the longitudinal direction of each slot with 0.8 mm cut-off and 4 mm evaluation length; then the average value was calculated to represent the surface roughness ( $R_a$  and  $R_z$ ) of each slot. Scanning Electron Microscope (SEM) was used to examine some selected machined workpieces for detailed analysis that reflects the results obtained in the line graphs. Machined workpieces were cleaned in distilled water inside an ultrasonic bath for 30 minutes and air-dried at ambient temperature to allow better surface measurements and observations. For SEM inspections, the glass samples were coated with OSMIUM layer with a thickness of 12 nm.

**Figure 2** Experimental setup (see online version for colours)

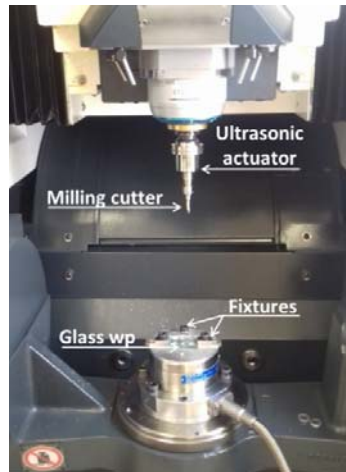


**Table 1** (a) Chemical composition and (b) mechanical properties of soda-lime glass

<i>Silica</i> <i>SiO<sub>2</sub></i>	<i>Soda</i> <i>Na<sub>2</sub>O</i>	<i>Lime</i> <i>CaO</i>	<i>Other</i> <i>additives</i>	<i>Density g/cm<sup>3</sup></i>	<i>Young's</i> <i>modulus GPa</i>	<i>Hardness</i>	<i>Poisson's</i> <i>ratio</i>
70%	15%	12%	3%	2.5	70	6	0.2

**Table 2** Diamond milling cutter specifications

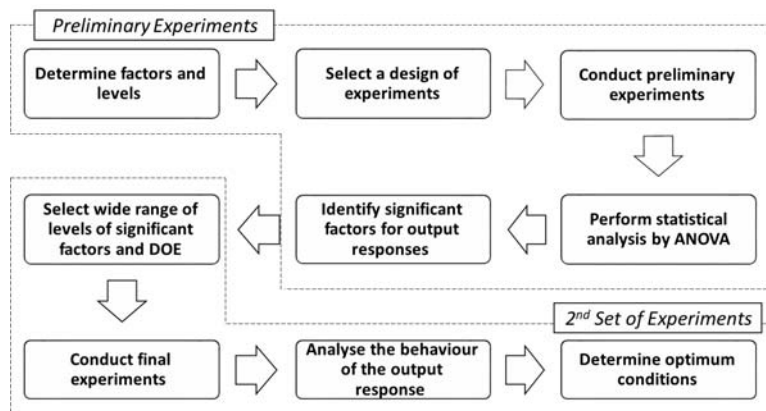
<i>Outer</i> <i>diameter <math>\phi</math></i> <i>OD (mm)</i>	<i>Wall</i> <i>thickness</i> <i>W (mm)</i>	<i>Diamond</i> <i>depth X</i> <i>(mm)</i>	<i>Grain</i> <i>size</i>	<i>Grain</i> <i>concentration</i>	<i>Ultrasonic</i> <i>frequency</i> <i>(kHz)</i>	<i>Bonding</i> <i>type</i>
4	1	8	D 64	N (50%c)	24.6	Galvanic
4	1	8	D 64	H (100%c)	25.4	Coated

### 3 Experimentation and data collection

#### 3.1 Preliminary experiments

Figure 3 explains the flow of the experimentation during this research. First, preliminary experiments were conducted using half fractional factorial design of experiments consisting of six factors (tool rotational speed, feed rate, depth of cut, ultrasonic vibration, grain structure, and cutting fluid) with two levels (low and high), each with two replications (Table 3). The main purpose of such group is to primarily investigate the most significant effect of the control variables and their interactions regarding the surface roughness. Minitab software (version 17) was used to generate the testing order as well as to assist in the statistical analysis of the experimental data. ANOVA results for each controllable factor on the surface roughness parameters ( $R_a$  and  $R_z$ ), resulting from the preliminary experiments, are shown in Table 4. Figure 4 defines the basic methodology of  $R_a$  and  $R_z$  measurements. Roughness average,  $R_a$ , is the arithmetic average of the absolute values of the profile heights over the evaluation length. Average maximum height of the Profile,  $R_z$  is the average maximum peak to valley of five consecutive sampling lengths within the evaluation length.

**Figure 3** Flowchart of the experimentation strategy

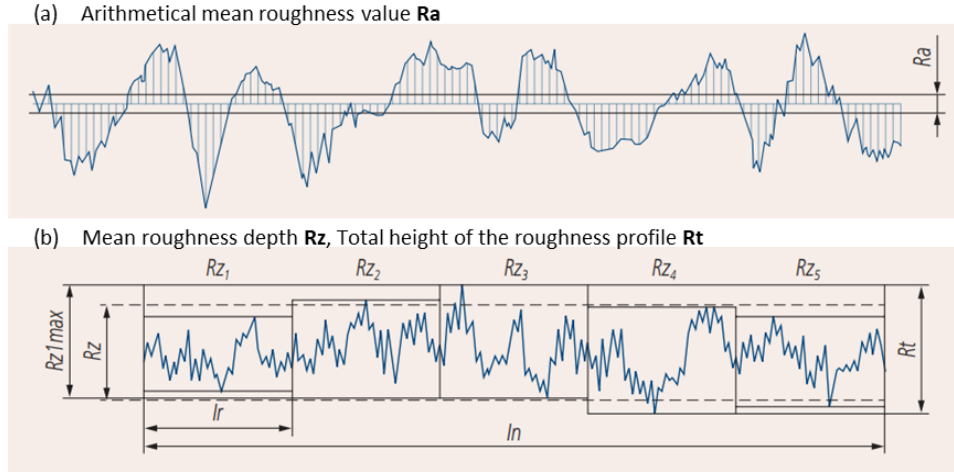


**Table 3** Cutting conditions of preliminary experiments

Factor	Label	Unit	Low level	High level
			(-1)	(+1)
Rotational speed	A	rpm	2000	10000
Feed rate	B	mm/min	10	100
Depth of cut	C	$\mu\text{m}$	20	100
Ultrasonic vibration	D	kHz	OFF	ON
Grain structure	E	%c	N	H
Cutting fluid	F	Internal	OFF	ON

**Table 4** ANOVA results for Ra and Rz

Factor	Ra					Rz						
	DoF	SS	MS	F-value	P-value	Contr. %	DoF	SS	MS	F-value	P-value	Contr. %
A (rpm)	1	0.67465	0.67465	15.82	0	11.4096	1	391.78	391.78	6.33	0.017	5.51197
B (mm/min)	1	1.56258	1.56258	36.65	0	26.4262	1	2963.3	2963.3	47.91	0	41.6908
C (µm)	1	0.34506	0.34506	8.09	0.007	5.83563	1	185.66	185.66	3	0.093	2.61206
D (US)	1	0.04776	0.04776	1.12	0.297	0.80771	1	1069.53	1069.53	17.29	0	15.0473
E (G.struc.)	1	0.23059	0.23059	5.41	0.026	3.89972	1	10.94	10.94	0.18	0.677	0.15392
F (C. fluid)	1	0.24135	0.24135	5.66	0.023	4.08169	1	127.66	127.66	2.06	0.16	1.79606
A*B	1	0.59627	0.59627	13.98	0.001	10.0841	1	5.51	5.51	0.09	0.767	0.07752
A*C	1	0.06322	0.06322	1.48	0.232	1.06917	1	5.87	5.87	0.09	0.76	0.08259
A*D	1	0.08054	0.08054	1.89	0.178	1.36209	1	34.99	34.99	0.57	0.457	0.49228
A*E	1	0.22387	0.22387	5.25	0.028	3.78607	1	70.86	70.86	1.15	0.292	0.99693
A*F	1	0.21959	0.21959	5.15	0.03	3.71369	1	2.6	2.6	0.04	0.839	0.03658
B*C	1	0.00002	0.00002	0	0.983	0.00034	1	148.72	148.72	2.4	0.131	2.09235
B*D	1	0.08747	0.08747	2.05	0.161	1.47929	1	266.33	266.33	4.31	0.046	3.74701
B*E	1	0.13203	0.13203	3.1	0.087	2.23288	1	0.25	0.25	0	0.949	0.00352
B*F	1	0.21123	0.21123	4.95	0.033	3.5723	1	13.18	13.18	0.21	0.647	0.18543
C*D	1	0.2865	0.2865	6.72	0.014	4.84526	1	28.8	28.8	0.47	0.5	0.40519
C*E	1	0.00148	0.00148	0.03	0.853	0.02503	1	415.43	415.43	6.72	0.014	5.84471
C*F	1	0.64454	0.64454	15.12	0	10.9004	1	2.3	2.3	0.04	0.848	0.03236
D*E	1	0.00316	0.00316	0.07	0.787	0.05344	1	31.49	31.49	0.51	0.481	0.44303
D*F	1	0.01327	0.01327	0.31	0.581	0.22442	1	158.04	158.04	2.55	0.119	2.22347
E*F	1	0.0763	0.0763	1.79	0.19	1.29038	1	50.75	50.75	0.82	0.372	0.714
Error	34	1.44966	0.04264				33	2041.27	61.86			
Pure error	26	0.9073	0.0349				27	1594.9	59.07			
Total	55	5.91299					54	7107.8				

**Figure 4** Surface roughness parameters (see online version for colours)

### 3.2 Second set of experiments

Based on the results of the preliminary experiments (Table 4), it can be concluded that the feed rate has the most significant effect on Ra and Rz; that are also influenced by the depth of cut, ultrasonic vibration, and cutting fluid usage. As the P-value is less than 0.05, then the factor is significant and vice versa; however, some significant factors has low contribution percentage because of its low corresponding degree of freedom (DOF = no. of levels – 1 = 2 – 1). Therefore, the rotational speed and grain concentration were eliminated as they had a minor influence on both Ra and Rz. In the present study, the arithmetic mean roughness (Ra) was selected to express the surface roughness, since it is the most widely used surface roughness parameter in industry to judge the surface quality. Based on the preliminary experiments, high rotational speed of 10,000 rpm and high grain concentration (100%*c*) were selected as lower surface roughness was obtained at these levels (Table 5). Therefore, the second group of experiments was conducted using general full factorial design of experiments with three replications to analyse the effect of the four selected significant factors on the surface roughness. Table 6 illustrates the machining conditions of the second group of experiments. Determination of the optimum conditions of UAM has been also discussed.

**Table 5** Preliminary experiments results for Ra and Rz

Mean value	Rotational speed (A)	Feed rate (B)	Depth of cut (C)	Ultrasonic vibration (D)	Grain structure (E)	Cutting fluid (F)
Ra <sub>bottom</sub>	↘	↗	↘	↗	↔	↘
Rz <sub>bottom</sub>	↘	↗	↘	↗	↘	↗



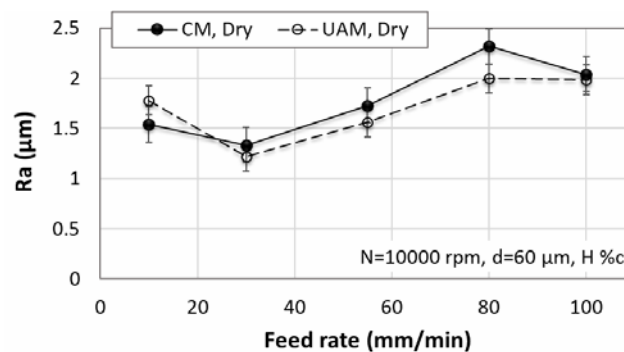
**Table 6** Cutting conditions of second group of experiments

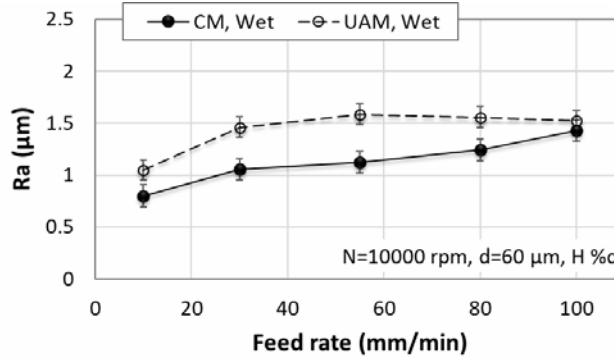
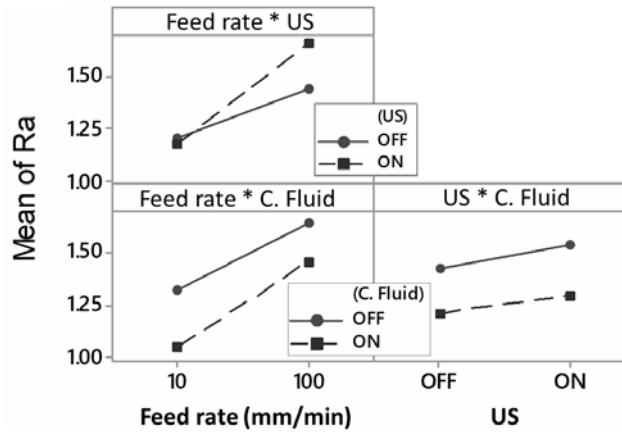
<i>Fixed factors:</i>						
<ul style="list-style-type: none"> <li>• Cutting tool [outer diameter (<math>\varnothing = 4</math> mm), wall thickness (<math>W = 1</math> mm), grain size D64]</li> <li>• Ultrasonic frequency: (<math>f = 25</math> kHz)</li> <li>• Ultrasonic amplitude: (<math>A = 5</math> <math>\mu\text{m}</math>)</li> <li>• Spindle rotational speed: (<math>N = 10,000</math> rpm)</li> <li>• Tool grain structure: H%c</li> </ul>						
<i>Factor</i>	<i>Unit</i>	<i>Levels</i>				
		<i>1</i>	<i>2</i>	<i>3</i>	<i>4</i>	<i>5</i>
Feed rate	mm/min	10	30	55	80	100
Depth of cut	$\mu\text{m}$	20	40	60	80	100
Ultrasonic vibration	0/kHz	Off	On			
Cutting fluid	On/Off	Off	On			

## 4 Results and discussion

### 4.1 Effects of feed rate

Figures 5 and 6 compare the effect of feed rate on Ra with and without ultrasonic assistance at dry and wet cutting conditions, respectively. The results show that Ra increases by increasing the feed rate even in case of CM and UAM or with/without cutting fluid. In UAM, it is clear that ultrasonic vibration slightly reduces the surface roughness Ra; in some conditions; by about  $\sim 10\%$  during dry machining. However, during wet machining, UAM produces higher values of Ra than that in CM. The reason for this is that, in UAM, the cutting tool is ultrasonically vibrated perpendicular to the milling surface. This axial vibration may increase the roughness of the machined surface through brittle fracture caused by the tool hammering effect. At dry cutting condition, Ra values are between  $1.2 \mu\text{m}$  and  $2.3 \mu\text{m}$  along the tested range of feed rates. However, using the cutting fluid positively improves the surface roughness, as Ra values are between  $0.8 \mu\text{m}$  and  $1.6 \mu\text{m}$ . These results justify the interaction effects of feed rate with ultrasonic assistance as well as the cutting fluid which are obtained from the preliminary experiments as shown in Figure 7.

**Figure 5** Effect of feed rate on Ra at CM and UAM without cutting fluid

**Figure 6** Effect of feed rate on Ra at CM and UAM with cutting fluid**Figure 7** Interaction effect of feed rate vs. ultrasonic assistance and cutting fluid on Ra

Figures 8(a) and 8(b) compare between the surface topography observed by SEM at different feed rates for both CM and UAM during dry and wet cutting, respectively. It can be seen that the brittle fracture mode of the glass material removed is common. As shown in Figures 8(a)-i and 8(a)-ii, in case of dry CM at low feed rate 10 mm/min and depth of cut 60  $\mu\text{m}$ , it is obvious that the machined surface is better than in case of dry UAM which shows more surface cracks. In UAM, the ultrasonic vibrating tool acts like a hammer which generates more cracks at the workpiece surface especially at low feed rate. By further increase of the feed rate, UAM slightly lowers Ra and gives a better surface finish. It is also clear that a lot of glass removed powder and chips covered the glass workpiece surface at dry cutting condition as shown in Figures 8(a)-iii and 8(a)-iv. During wet cutting conditions, it is evident that CM [Figures 8(b)-i and 8(b)-iii] produces surface with more smooth areas than UAM [Figures 8(b)-ii and 8(b)-iv] due to the hammering effect of the vibrated tool occurring in case of UAM. Figure 9 shows the surface features at severe cutting conditions of feed rate 100 mm/min, CM, and dry cutting. Under these conditions, the surface is exposed to high cutting forces. Lays are also observed on the workpiece surface as shown in Figure 9(a). The removed glass powder has adhered to the workpiece surface in some areas with some grains pulled out from the cutting tool and stacked on it, Figures 9(b) and 9(c). Additionally, some long

cracks and workpiece surface separation are found in Figure 9(d). The high feed rate results in high friction between the cutting tool and the workpiece surface that deteriorates the surface finish. In addition, the continuous contact between the cutting tool and the workpiece surface results in high heat generation in the machining zone during dry CM. These results can be summarised as that; the surface roughness Ra is increased by increasing the feed rate. Better surface finish is obtained when using the cutting fluid which helps in removing the debris and chips produced during machining. UAM slightly lowers the surface roughness, at some levels of feed rate, during dry condition. However, wet CM gives better surface at lower level of feed rate than UAM.

**Figure 8** Surface topography comparison: feed rate vs. ultrasonic assistance at (a) dry and (b) wet cutting

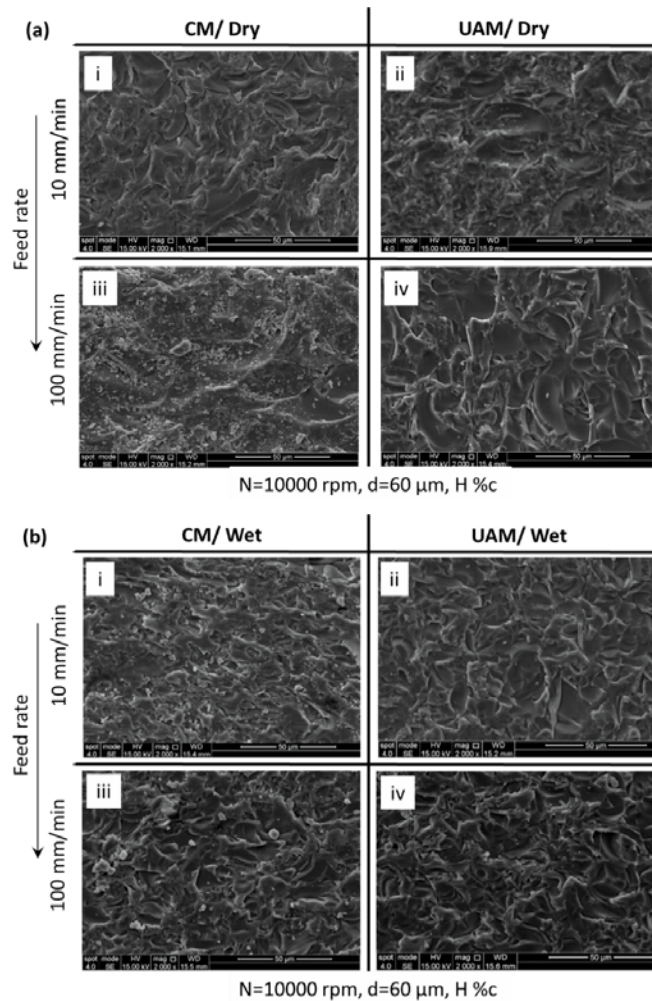
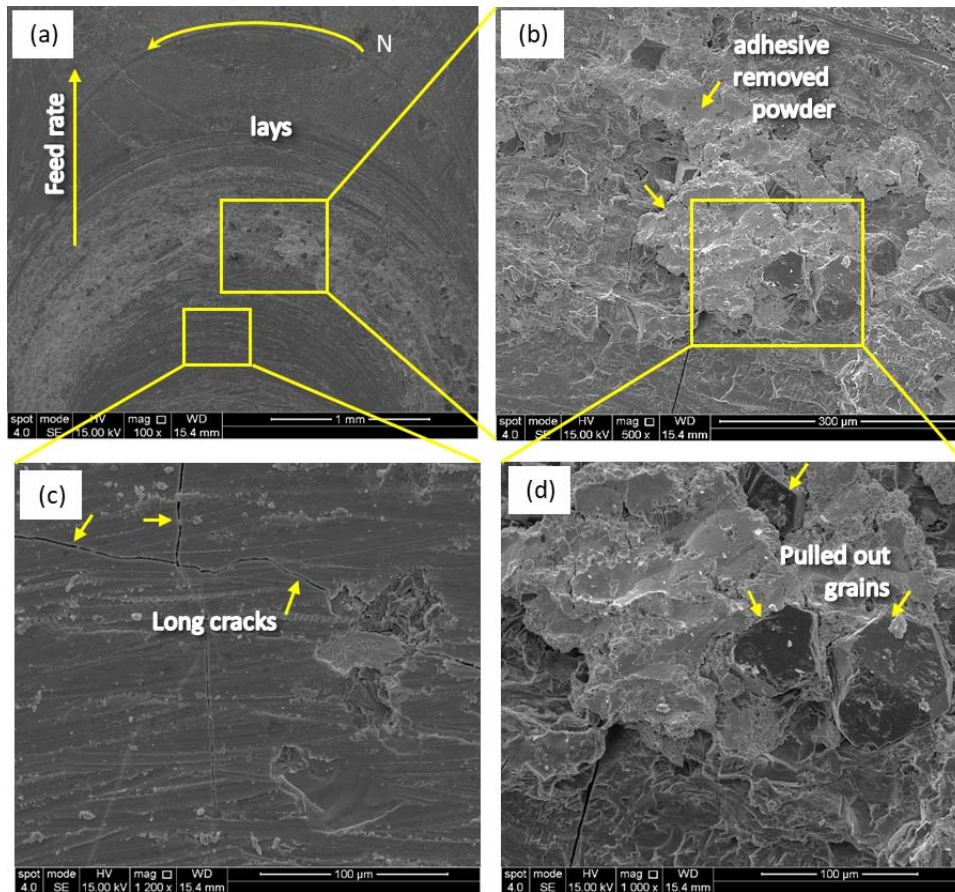


**Figure 9** Surface topography at high feed rate (100 mm/min), and dry CM (see online version for colours)



#### 4.2 Effects of depth of cut

Figures 10 and 11 compare the effect of depth of cut on  $R_a$  during CM and UAM at dry and wet cutting conditions, respectively. Contrary to expectations, the results show that; the general trend of decreasing  $R_a$  with increasing the depth of cut for both CM and UAM, and at dry or wet cutting conditions is related to the pulverisation phenomenon, see Figures 12 and 13. As the cutting tool used in this study is a bonded diamond abrasive one, so the removed glass material is a powder-like or dust. By increasing the depth of cut, the amount of this powder is increased and accumulated underneath the tool end face, which is rotated and fed toward the workpiece. Thus, the removed glass powder accumulated under the tool end face acts like pulverisation or additional grinding of the machined surface.

**Figure 10** Effect of depth of cut on Ra at CM and UAM without cutting fluid

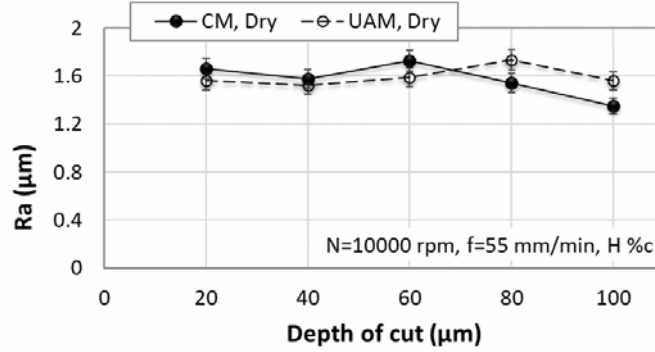


**Figure 11** Effect of depth of cut on Ra at CM and UAM without cutting fluid

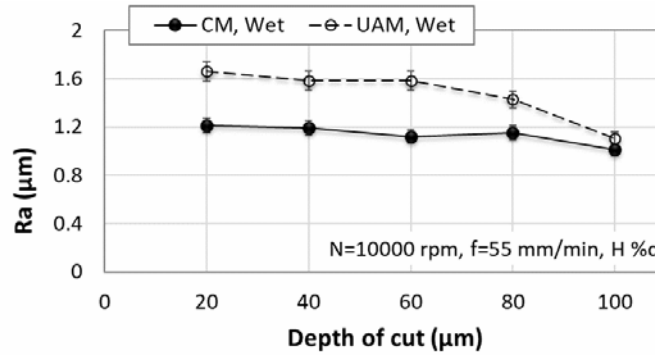


**Figure 12** Mechanism of pulverisation

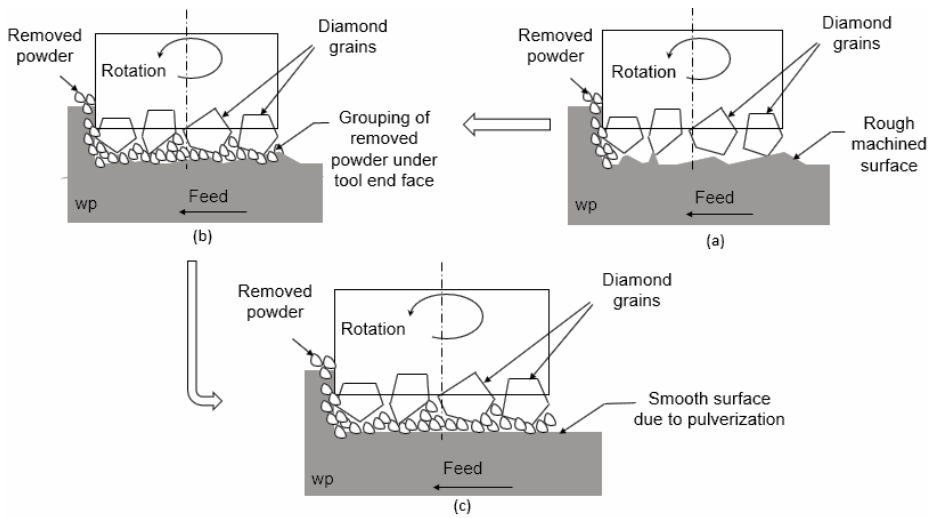


**Figure 13** Powder of removed glass stacked on the workpiece surface and the cutting tool (see online version for colours)

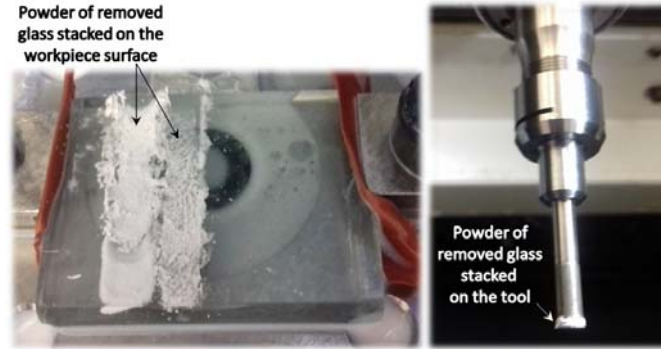
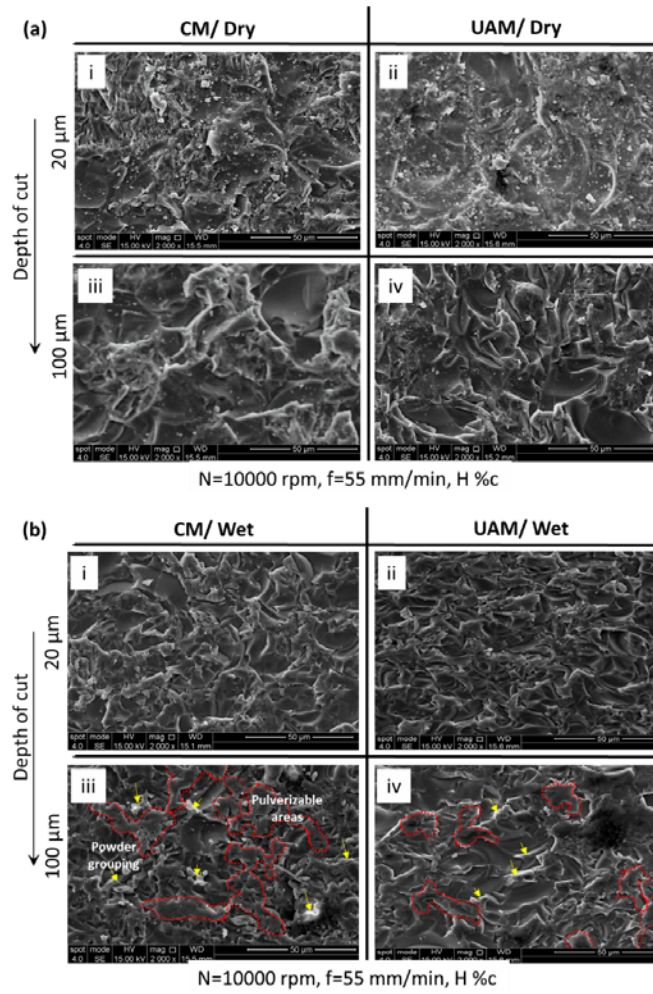
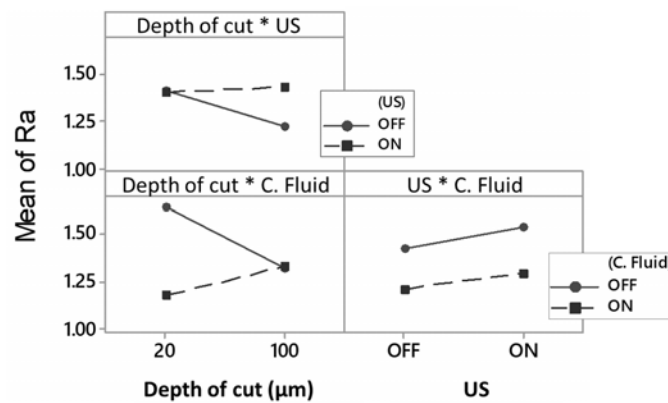


**Figure 14** Surface topography comparison: depth of cut vs. ultrasonic assistance at (a) dry and (b) wet cutting (see online version for colours)



SEM images of the surface topography at different depths of cut are shown in Figures 14(a) and 14(b) for both CM and UAM during dry and wet cutting, respectively. At low depth of cut of 20  $\mu\text{m}$  and feed rate of 55 mm/min during CM and UAM, Figures 14(a)-i and 14(a)-ii, the glass powder and chips removed are obvious on the surface. However, more cracks are observed in case of CM than UAM. At high depth of cut of 100  $\mu\text{m}$ , Figures 14(a)-iii and 14(a)-iv clarify the pulverised areas which lead to lower surface roughness especially in case of CM. During wet cutting, it is noticeable that Ra is lower in case of CM [Figures 14(b)-i and 14(b)-iii] than UAM [Figures 14(b)-ii and 14(b)-iv]. Beside the pulverisation effect, the longitudinal vibration and the hammering action of the cutting tool in UAM may cause micro-damage and cracks onto the workpiece surface, resulting in increasing the surface roughness. The results also show that using of the cutting fluid leads to lower surface roughness values during CM which range from 1  $\mu\text{m}$  to 1.2  $\mu\text{m}$ . However, Ra values range between 1.35  $\mu\text{m}$  to 1.7  $\mu\text{m}$  during dry CM or dry UAM. These results justify the interaction effects of depth of cut with ultrasonic assistance and with cutting fluid which are obtained from the preliminary experiments as shown in Figure 15. Along these results, it can be concluded that higher depth of cut results in lower surface roughness Ra, because of the pulverisation phenomenon. In addition, better surface finish is obtained during wet CM than UAM.

**Figure 15** Interaction effect of depth of cut vs. ultrasonic assistance and cutting fluid on Ra



### 4.3 Parameters optimisation

Contour plots have been used to check the effectiveness of the statistical analysis of the results and fulfil the desirable response values at machining conditions. The target for surface roughness optimisation is to minimise Ra. The four plots shown in Figure 16 present the contour graphs for Ra with varying feed rate, depth of cut, ultrasonic assistance, and cutting fluid. Blue areas indicate lower surface roughness and the dark green areas indicate higher surface roughness. Figure 16(a), at CM and dry cutting, Ra is lower than 1.5  $\mu\text{m}$  at feed rate 10:20 mm/min and depth of cut 70:100  $\mu\text{m}$ . Figure 16(b), UAM and dry cutting, Ra is between 1.3:1.4  $\mu\text{m}$  at feed rate 10:20 mm/min and almost all levels of depth of cut. Figure 16(c), CM and wet cutting, Ra is lower than 0.7  $\mu\text{m}$  at a feed rate of 10 mm/min and depth of cut 90:100  $\mu\text{m}$ . Figure 16(d), UAM and wet cutting, Ra value is between 1:1.1  $\mu\text{m}$  at feed rate 10:20 mm/min and depth of cut 80:100  $\mu\text{m}$ .

Therefore, it can be concluded that the best combination of cutting conditions that achieves minimum value of Ra is obtained in Figure 16(c). A response optimiser has been used in order to obtain the optimal cutting conditions for minimising Ra. As shown in Figure 17, the optimal conditions that minimise Ra are at feed rate 10 mm/min, depth of cut 100 µm, without ultrasonic assistance, and when using cutting fluid, which give Ra ≈ 0.64 µm.

**Figure 16** Contour plots for Ra vs. feed rate and depth of cut, (a) CM+dry (b) UAM+dry (c) CM+wet (d) UAM+wet (see online version for colours)

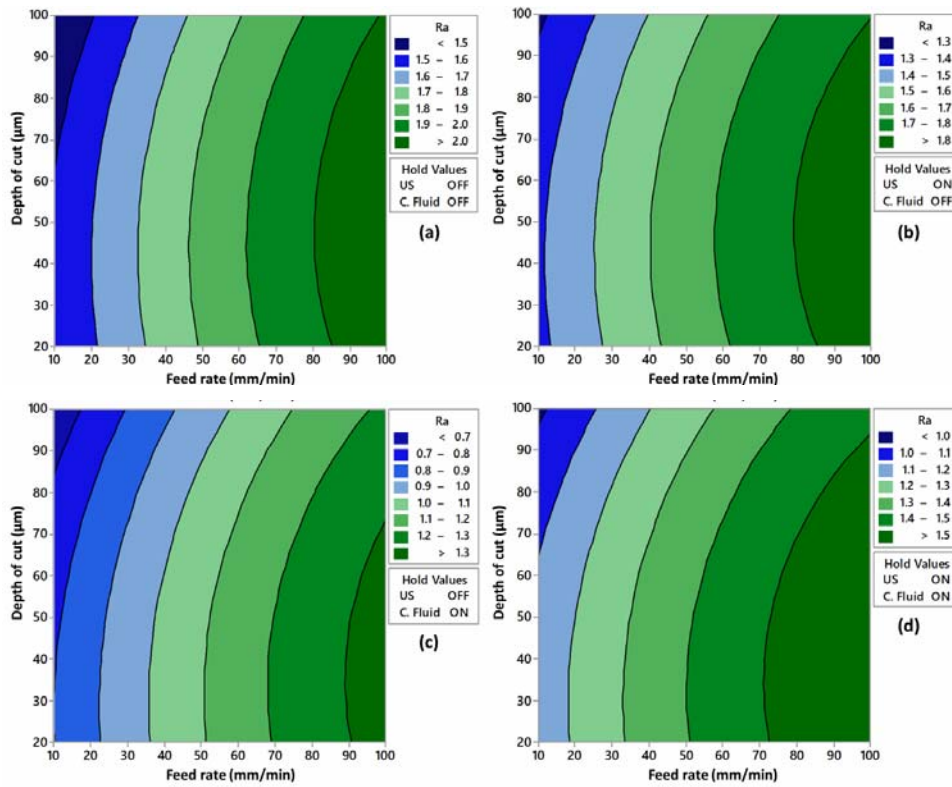
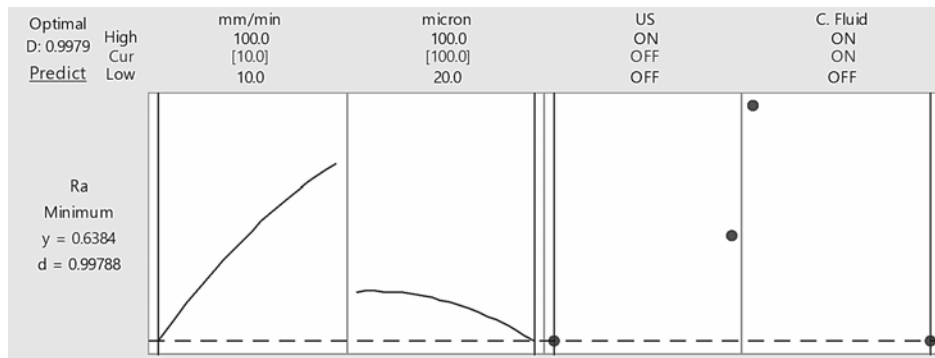


**Figure 17** Optimisation plot for Ra





## 5 Conclusions

Based on the analysis and observations of the experimental results for UAM and CM of soda-lime glass, the following conclusions are drawn:

- The tool feed rate is the most influential variable for the surface roughness parameters (Ra and Rz) in both UAM and CM and that increasing the feed rate leads to higher values of surface roughness.
- The surface roughness is decreased when the depth of cut is increased which can be attributed to the pulverisation phenomenon.
- Cutting fluid lowers the surface roughness and improves the machined surface finish compared to dry cutting for both UAM and CM. Cutting fluid removes the debris and swarf from the machining area at faster rate leading to finer machined surface.
- UAM slightly lowers the surface roughness between 5 to 10% compared with CM in some conditions of medium to high feed rate and depth of cut during dry cutting. However, UAM produces rougher surface with about 25% higher than CM during wet cutting.
- For minimum surface roughness, the parametric combination has been attained as feed rate of 10 mm/min, depth of cut of 100  $\mu\text{m}$ , during wet CM at fixed spindle speed of 10,000 rpm and high grain concentration.

## References

- Abd Halim, F.N.H., Ascroft, H. and Barnes, S. (2017) 'Analysis of tool wear, cutting force, surface roughness and machining temperature during finishing operation of ultrasonic assisted milling (UAM) of carbon fibre reinforced plastic (CFRP)', *Procedia Engineering*, Vol. 184, pp.185–191, doi: 10.1016/j.proeng.2017.04.084.
- Abdo, B., Darwish, S.M. and El-Tamimi, A.M. (2012) 'Optimization of process parameters of rotary ultrasonic machining based on Taguchis method', *Applied Mechanics and Materials*, Vols. 184–185, pp.11–17, doi: 10.4028/www.scientific.net/AMR.748.273.
- Amin, M., Yuan, S., Khan, M.Z., Zhen, L., Nawaz, M.K. and Wu, Q. (2017) 'Modeling and optimization for rotary ultrasonic face milling of carbon fiber reinforced polymers', *MATEC Web Conf.*, doi: 10.1051/mateconf/201710402017.
- Babuji, C., Kumar, N.S., Vijayan, K., Rao, G.N. and Chaman, J.J. (2017) 'Effect of machining parameters on surface roughness and material removal rate during rotary ultrasonic machining', *International Research Journal of Engineering and Technology (IRJET)*, Vol. 4, No. 6, pp.2324–2329 [online] <https://irjet.net/archives/V4/i6/IRJET-V4I6453.pdf>.
- Dambon, O., Klocke, F., Heselhans, M., Bulla, B., Weber, A., Schug, R. and Bresseler, B. (2007) 'Vibration-assisted machining research at Fraunhofer IPT – diamond turning and precision grinding', *American Society of Precision Engineering*, pp.3–10.
- Feucht, F., Ketelaer, J., Wolff, A., Mori, M. and Fujishima, M. (2014) 'Latest machining technologies of hard-to-cut materials by ultrasonic machine tool', *Procedia CIRP*, Vol. 14, pp.148–152, Elsevier B.V., doi: 10.1016/j.procir.2014.03.040.
- Hamzah, E., Sudin, I., Khoo, C-Y., Abidin, N.N.Z. and Tan, M.J. (2008) 'Effect of machining parameters on BK7 optical glass using conventional and rotary ultrasonic machines', *Journal of the Japanese Society for Experimental Mechanics*, Vol. 8, pp.127–132.

- Hu, Y., Wang, H., Ning, F., Cong, W. and Li, Y. (2017) 'Surface grinding of optical BK7/K9 glass using rotary ultrasonic machining: an experimental study', *Proceedings of the ASME – 12th International Manufacturing Science and Engineering Conference*, Los Angeles, CA, USA, doi: 10.1115/MSEC2017-2780.
- Jiang, C., Wang, C. and Li, H. (2016) 'Experimental investigation of brittle material removal fraction on an optical glass surface during ultrasound-assisted grinding', *International Journal of Advanced Manufacturing Technology*, Vol. 86, Nos. 1–4, pp.419–426, doi: 10.1007/s00170-015-8215-7.
- Jiao, Y., Hu, P., Pei, Z.J. and Treadwell, C. (2005) 'Rotary ultrasonic machining of ceramics: design of experiments', *Int. J. Manufacturing Technology and Management*, Vol. 7, Nos. 2–4, pp.192–206.
- Klocke, F., Soo, S.L., Karpuschewski, B., Webster, J.A., Novovic, D., Elfizy, A., Axinte, D.A. and Tönissen, S. (2015) 'Abrasive machining of advanced aerospace alloys and composites', *CIRP Annals – Manufacturing Technology*, Vol. 64, No. 2, pp.581–604, doi: 10.1016/j.cirp.2015.05.004.
- Kumar, M.N. et al. (2014) 'Vibration assisted conventional and advanced machining: a review', *Procedia Engineering*, Vol. 97, pp.1577–1586, Elsevier B.V., doi: 10.1016/j.proeng.2014.12.441.
- Kuo, K.L. (2008) 'A study of glass milling using rotary ultrasonic machining', *Key Engineering Materials*, Vol. 364–366, pp.624–628, doi: 10.4028/www.scientific.net/KEM.364-366.624.
- Lee, M.H. et al. (2008) 'Parameters optimization of rotary ultrasonic machining of glass lens for surface roughness using statistical Taguchi's experimental design', *Proceedings of the 13th WSEAS International Conference on Applied Mathematics (MATH'08)*, pp.214–219.
- Ning, F. et al. (2017) 'Rotary ultrasonic surface machining of CFRP composites: a comparison with conventional surface grinding', *Procedia Manufacturing*, Vol. 10, pp.557–567, Elsevier B.V., doi: 10.1016/j.promfg.2017.07.049.
- Singh, R.P. and Singhal, S. (2017) 'Rotary ultrasonic machining of macor ceramic: an experimental investigation and microstructure analysis', *Materials and Manufacturing Processes*, Vol. 32, No. 9, pp.927–939, doi: 10.1080/10426914.2016.1198033.
- Suárez, A. et al. (2016) 'Effects of ultrasonics-assisted face milling on surface integrity and fatigue life of Ni-Alloy 718', *Journal of Materials Engineering and Performance*, Vol. 25, No. 11, pp.5076–5086, doi: 10.1007/s11665-016-2343-6.
- Uhlmann, E. and Hübert, C. (2007) 'Ultrasonic assisted grinding of advanced ceramics', *American Society of Precision Engineering*, pp.43–47.
- Wang, H., Cong, W., Ning, F. and Hu, Y. (2017) 'A study on the effects of machining variables in surface grinding of CFRP composites using rotary ultrasonic machining', *The International Journal of Advanced Manufacturing Technology*, doi: 10.1007/s00170-017-1468-6.